

Copolymerization of Biomass-Derived Carboxylic Acids for Biobased Acrylic Emulsions

Ashish Bohre,^{*,†} Mohammad Asif Ali,[‡] Martin Ocepek,[§] Miha Grilc,[†] Jožefa Zabret,[§] and Blaž Likozar^{*,†}

[†]Department of Catalysis and Chemical Reaction Engineering, National Institute of Chemistry, Hajdrihova 19, 1000 Ljubljana, Slovenia

[‡]Soft Matter Sciences and Engineering Laboratory, ESPCI Paris, PSL University, CNRS, 10 rue Vauquelin, 75005 Paris, France

[§]Helios TBLUS d.o.o., Količevo 65, 1230 Domžale, Slovenia

Supporting Information

ABSTRACT: The production of biobased copolymers such as poly(styrene-*co*-butyl acrylate-*co*-methacrylic acid) for paints and coating applications is indispensable for the establishment of sustainable biorefineries, but it is challenging because of the utilization of fossil-based sources for the syntheses of methacrylic acid (MAA) from biomass. We have studied the catalytic decarboxylation of biobased itaconic acid, citric acid, and aconitic acid to MAA. Among different tested catalysts, the spinel BaAl₁₂O₁₉ chemical substance was found to grant an additional active catalysis, it optimized selectivity, and a 50% synthesis yield of MAA was achieved. The as-synthesized MAA vinyl monomer has been consequently utilized for the production of a chain-growth poly(St-*co*-BA-*co*-MAA) copolymer, industrially manufactured for coating, adhesive, and paint end-user applications. The latexes' physical properties of bio-MAA-incorporated structured polymers have also been compared with a copolymerized commercial poly(St-*co*-BA-*co*-MAA) terpolymer, fabricated from petroleum-based MAA. The functional group distribution, measured molecular weight (M_w), determined polydispersity index (\mathcal{D}_M), glass transition temperature (T_g), and integrated solid content (w_s) of copolymerization poly(St-*co*-BA-*co*-MAA) constituent units were comparable with benchmarks.



1. INTRODUCTION

The copolymers of styrene (St) and *n*-butyl acrylate (BA) are important polymeric materials commercially utilized for the production of adhesive, coating materials, and paint because of its excellent physical and chemical properties.^{1,2} The latex paints produced from these copolymers exhibited resistance to weathering and long-lasting color.³ These copolymers are industrially synthesized by emulsion polymerization, that is an extensively used process for manufacturing synthetic polymers today.⁴ However, the final product produced from this method exhibited poor optical and thermal resistance.⁵

During the emulsion polymerization process, acrylic acid and methacrylic acid (MAA) are added to enhance their latex properties. It can also make the copolymer pH resistant, thermal resistant, and improve their mechanical and adhesive properties.^{7,8} The presence of the carboxylic group on the outer surface provides stability to the poly(St-*co*-BA-*co*-carboxylic acid) copolymer.^{9,10} The main disadvantage associated with the use of such carboxylic acids is the source of origin. Industrially these monomers are derived from fossil-based sources that are finite in nature.¹¹ The transition from petrol-based to bio-based coating materials is of general interest to achieve sustainability. However, technical and economic drawbacks slow down this transition.¹²

Numerous research works have been done recently to find feasible solutions in the academic area. On the other hand, not many generated knowledge was transferred to conventional coating business. Meeting harsh legislation requirements in some countries is the main driving force for development and scale-up of (partly) biobased coatings.¹³ There are several known paths to produce bio acrylic acid.¹¹ On the other hand, commercially available methacrylates are so far almost exclusively petrol based.

MAA is an industrially important versatile monomer currently produced by the acetone cyanohydrin process.^{14–16} However, because of the utilization of unsustainable feedstocks, processing of waste acid was problematic.¹⁷ To sort out the aforementioned issues, an improved version was patented in 1997.¹⁸ This improved process did not require the addition of mineral acids, and hydrogen cyanide can be recycled. However, the short lifetime of the catalyst and production of excess amount of side products render the commercialization of this process.^{19–21}

Received: July 24, 2019

Revised: October 3, 2019

Accepted: October 9, 2019

Published: October 9, 2019

Itaconic acid (IA) and citric acid are industrially important commodity chemicals produced by the fermentation of biomass.^{22,23} Interestingly, St and BA can also be obtained through biomass-derived sugars and biobutanol, respectively.^{24,25}

Heterogeneous catalysts supported on noble metals (Pd/C, Pd/Al₂O₃, Pt/C, Pt/Al₂O₃, and Ru/C) have also been developed for the production of MAA by using IA as the feedstock.²⁰ A good yield (68%) of MAA was attained under relatively mild temperature and pressure conditions with Pt/Al₂O₃. However, this process required subsequent addition of corrosive sodium hydroxide that makes this process unsustainable. Additionally, the utilization of noble metal-based catalyst is not cost competitive. Later, Pirmoradi and Kastne employed a hydroxalcalite catalyst and achieved only 23% yield of MAA from IA.²¹

In collaboration with HELIOS, one of the world's leading paint and coating producers, we describe an effective strategy for the production of biobased poly(St-co-BA-co-MAA) copolymers by adopting a two-step approach. In the first step, various heterogeneous catalysts have been tested for the production of MAA. In the second step, poly(St-co-BA-co-MAA) copolymers have been prepared by the radical polymerization of as-synthesized MAA with St and BA.

2. EXPERIMENTAL SECTION

2.1. Catalyst Synthesis. The BaAl₁₂O₁₉ catalyst was synthesized by the previously reported method.²⁶ In a typical procedure, stoichiometric amounts of barium nitrate (90.03 g) and aluminium nitrate (5.23 g) were mixed in hot distilled water (100 mL) to get a clear solution. In this solution, carbon black (40 g) was added with constant stirring and kept overnight. Next, the aqueous solution of ammonium carbonate (96.09 g) was added dropwise into the mixture for 4 h to produce a gel that was subsequently washed with distilled water and dried at 110 °C in an oven for 12 h. Finally, calcination of the obtained white powder was performed at 1250 °C in argon for 5 h. The deposited carbon from the as-prepared catalyst was removed by calcination of the catalyst at 900 °C for 12 h in air. MgAl₂O₄, NaAl₂O₄, and CaAl₂O₄ were also prepared from the above-mentioned method.

Pd/BaAl₁₂O₁₉, Pd/MgAl₂O₄, Pd/NaAl₂O₄, and Pd/ZrO₂ catalysts with 5 wt % metal loading were prepared by the deposition–precipitation method. Typically, 1 g of the support was dissolved in the aqueous solution of Pd(NO₃)₂. Next, NH₄OH was added until the pH reached to 9 followed by stirring of the reaction mixture at 60 °C for 1 h. The obtained support was filtered and washed with distilled water followed by drying at 60 °C for 12 h. Finally, the dried materials were reduced in a H₂ flow at 350 °C for 3 h. The CaMgO catalyst was synthesized as per the method described in the literature.²⁷

2.2. Catalyst Characterization. X-ray diffraction (XRD) measurements were conducted on a PANalytical X'Pert PRO diffractometer with a Cu K α ($\lambda = 1.5405 \text{ \AA}$) radiation source. N₂-physisorption measurements were performed on a Micromeritics ASAP 2020 system. Temperature programmed desorption was performed by using a chemisorption analyzer (Micromeritics 2920 AutoChem II) with a mass-spectrometry detector. The morphology of the materials was observed by using a JEOL, JEM-ARM200CF system equipped with a JEOL Centurio 100 mm² energy-dispersive X-ray spectroscopy system.

2.3. Catalytic Activity Measurement. Catalytic reactions were performed in a Parr reactor. Typically, 2 g of IA and 1 g of catalyst were added in 100 mL of distilled water and loaded into the autoclave reactor. The reactor was sealed, purged three times with N₂, and the desired pressure was adjusted. Finally, the reactor was stirred (600 min⁻¹) and heated up to the desired temperature and time. When reaction completed, the reactor was cooled at room temperature, the pressure was released, and crude reaction mixture was analyzed by high-performance liquid chromatography (HPLC).

2.4. MAA Extraction and Purification Procedure. The purification of crude MAA was performed by following the reported method.²⁰ In a typical procedure, the crude MAA was added in a separating funnel and extracted by the addition of Et₂O (3 \times 50 mL). The obtained Et₂O solution was evaporated under reduced pressure to get purified MAA. The purity and structure of the isolated MAA were determined by NMR spectroscopy. The obtained ¹H and ¹³C NMR spectra confirmed the extraction of purified MAA with 99.0% purity (Figures S3 and S4).

2.5. Syntheses of Copolymers. Polymerizations were carried out in an Optimax (Mettler Toledo) synthesis station equipped with a mechanical stirrer (4 pitched blade turbine shape) and a purge condenser for nitrogen equipped with a thermocouple. In a typical procedure, butyl acrylate (BA) (53.29 g) and butyl acetate (76.10 g) were added in a 150 mL round-bottom Schlenk vessel containing styrene (9.57 g). The mixture was stirred at room temperature to dissolve butyl acrylate and butyl acetate in styrene. Next, peroxybenzoate (0.330 g) and MAA (1.0 g) were added to the flask with continuous stirring. The mixture was degassed by three freeze-pump-thaw cycles, back-filled with nitrogen, and placed in an oil bath, followed at 125 °C for 4 h. During the polymerization after 2 h, the postpolymerization was carried out by adding butyl acrylate (3.10 g) and *tert*-butyl peroxybenzoate (0.18 g) as the initiator, and reaction vessel was placed in an ice bath to stop the polymerization.

2.6. Characterization of Copolymers. Gel permeation chromatography (GPC) was carried out on a Waters 2690 Separations Module, coupled with a Waters 410 differential refractometer (RID). Samples were dissolved in tetrahydrofuran 0.0025 g mL⁻¹. After 3 days, solutions were filtered through a 0.45 μ m filter, and 100 μ L was injected. A Series of three Styragel columns (HR 4E, HR 5E, and HR 0.5) was used. The average molecular weight was calculated according to polystyrene standards with the use of manufacturer software.

FT-IR Nicolet 6700, Thermo Scientific, was used to obtain Fourier transformed infrared spectra (FT-IR). Samples were applied in a thin layer on a KBr pellet and let to dry. The pellet was then inserted, and spectra in the range 400–4000 cm⁻¹ were collected. Volatile compounds were analyzed with the use of an Agilent 6890N Gas chromatograph (capillary column HP-5MS UI, helium as carrier gas), coupled with mass selective detector Agilent 5973. Samples were dissolved in methylene chloride; *n*-heptane was added as the internal standard. Solutions were ultrasonically mixed for 5 min. One milliliter of the sample was analyzed. Content of each volatile substance was calculated according to premeasured standards.

Glass transition temperatures (T_g) and thermogravimetric analysis (TGA) were obtained by Mettler Toledo TGA/DSC 1. Spectra were analyzed with manufacturer software. For differential scanning calorimetry (DSC) analysis, the dried samples were weighted and heated (ramp 10 °C min⁻¹) in the

range of -50 to 150 °C. The results of T_g are reported as an inflection point value. The total solid content was determined gravimetrically. Polymer solutions (1–1.5 g) were weighted into aluminum dishes and put in the oven for 1 h at 125 °C. Dynamic rheological tests were carried out using a rotational rheometer (Anton Paar Physica MCR 301), equipped with fixture PP25 parallel-plate geometry. The shear rate range was 0.01 – 100 s^{-1} . The acid number was determined by titration using 0.1 M KOH, according to ISO 2114.

3. RESULTS AND DISCUSSION

3.1. Catalytic Synthesis of Biobased Methacrylic Acid.

It is known from the literature that the noble metal-loaded catalyst exhibited good yield and selectivity toward MAA.²⁰ In the initial experiments, we have prepared and tested a variety of noble metal (Pd, Pt, and Ru) supported heterogeneous catalysts for the decarboxylation of IA to MAA with water as the solvent, using 20 bar N_2 at 250 °C for 3 h. The detailed characterizations of the as-synthesized catalysts are available in the Supporting Information

First, we have performed the screening of the active noble metal for the synthesis of MAA from IA (Table 1, entry 1–3).

Table 1. Screening of Pd and Pt-Based Catalysts for the Decarboxylation of Itaconic Acid

entry ^a	catalyst	conversion (%)	selectivity (%)
1	Pd/C	95	32
2	Pt/C	100	25
3	Ru/C	90	1
4	Pd/Al ₂ O ₃	97	29
5	Pd/SiO ₂	93	25
6	Pd/ZrO ₂	87	12
7	Pd/BaSO ₄	91	34
8	Pd/MgAl ₂ O ₄	100	17
9	Pd/CaAl ₂ O ₄	94	40
10	Pd/BaAl ₁₂ O ₁₉	100	46

^aReaction conditions: IA, solvent (water, 150 mL), time (3 h), catalyst (1 g, 5 wt % of the metal), and values were determined by HPLC.

The reactivity of the Pd/C catalyst is higher than those of Pt/C and Ru/C catalysts, which can be attributed to the positive stabilization effect of the palladium metal on the itaconate monoanion that promotes the decarboxylation of IA to MAA.²⁰ Interestingly, Ru/C catalysts showed totally different activity with the low MAA yield (1%) and high conversion of IA (90%) probably because of the deoxygenation of IA and MAA. It was confirmed from the initial experiments that palladium is an active metal for the catalytic conversion of IA to MAA.

In the next set of experiments, we have tested variety of Pd-based catalysts (Table 1, entry 4–10). The selectivity of MAA significantly varied for different catalyst supports. The catalytic activities of acidic supports such as ZrO₂, SiO₂, and Al₂O₃ were lower than the basic support and spinels of MgAl₂O₄, BaAl₁₂O₁₉, and CaAl₂O₄ supports (Table S1). The high acidity of the catalysts promotes the hydration of IA to citramalic acid. The further degradation of citramalic acid produced 2-hydroxyisobutamic acid (2-HIBA) and pyruvic acid; hence, this reduced the overall yield of MAA.^{19,21} De Schouwer et al. recently reported that the catalysts can alter the pH of the reaction mixture. For instance, the Pd/ZrO₂ catalyst yielded a

pH of 3.7, and Pd/CaAl₂O₄ and Pd/BaAl₁₂O₁₉ yielded neutral pH, whereas the Pd/MgAl₂O₄ catalyst yielded a pH of 8.9, which was obtained when suspended in H₂O and stirred for 6 h.²⁸ It was reported in the literature that low or high pH of the reaction mixture promotes the parasitic reaction pathways and produced undesired side products such as acetic acid, acetone, 2-HIBA, and so forth.¹⁴

To investigate the effect of catalyst acidity and basicity on the MAA yield, we have prepared variety of acidic and basic catalysts. We have started our investigation with heterogeneous base catalysts (Table 2). It was observed that the catalyst with

Table 2. Screening of Heterogeneous Catalysts for the Decarboxylation of Itaconic Acid

entry ^a	catalyst	conversion (%)	selectivity (%)
1	CaMgO	97	33
2	NaAl ₂ O ₄	100	34
3	CaAl ₂ O ₄	100	36
4	BaAl ₁₂ O ₁₉	100	50
5	MgAl ₂ O ₄	100	26
6	BEA-300	100	28
7	HY-30	97	25
8	HY-80	94	23
9	ZSM5-30	91	21
10	Amberlyst-15	87	17

^aReaction conditions: IA, solvent (water, 150 mL), time (3 h), catalyst (1 g), and values were determined by HPLC.

high Brønsted basic sites exhibited poor MAA selectivity. For example, the CaMgO catalyst having high basicity (Table S2) yielded MAA with 33% selectivity (Table 2, entry 1). Similar results were obtained when other Brønsted base catalysts such as NaAl₂O₄ and CaAl₂O₄ were tested (Table 2, entry 2–3). Delightedly, we found that the spinel BaAl₁₂O₁₉ catalyst showed good MAA selectivity (50%) with complete conversion of IA (Table 2, entry 4). However, slightly basic MgAl₂O₄ catalyst showed relatively low MAA selectivity (Table 2, entry 4).

Next, we have used variety of acidic zeolites and Amberlyst-15 catalyst (Table 2, entry 5–10). It was found that the selectivity of the MAA is inversely proportional to the acidity of the catalysts. Amberlyst-15 with high Brønsted acid density demonstrated poor activity with $\sim 17\%$ selectivity to MAA (Table 2, entry 10). Whereas, the selectivity of MAA was partially increased when moderate acidic zeolites were utilized for the decarboxylation of IA (Table S2, entry 7–10). It was concluded from our experiments that high acidity or basicity of the catalyst reduces the yield of MAA by subsequent decarboxylation and hydration reactions. Compared to the tested catalysts, the outstanding catalytic activity of BaAl₁₂O₁₉ is because of their large surface area, modest basicity, and the peculiar-layered structure that promotes the decarboxylation reaction (Table S2, entry 4).²⁹

Impurities present in the MAA monomer played a vital role that can alter the properties of the prepared copolymer. We have detected 2-HIBA as a major side product in the crude reaction mixture along with the traces of acetic acid and pyruvic acid. 2-HIBA is produced from the hydration of MAA that further degraded into pyruvic acid and acetic acid. With the aim to obtain purified MAA, we have performed the distillation and solvent extraction process, as reported by Le Nôtre et al. in 2014.²⁰ As confirmed by the ¹H and ¹³C NMR

spectrums of purified MAA (Figures S3 and S4), we have isolated 99.0% pure MAA from the crude reaction mixtures by following this process.

In the final approach, the scope of the as-synthesized $\text{BaAl}_{12}\text{O}_{19}$ catalyst was further extended toward other biomass-derived carboxylic acids, and the results are shown in Table 3.

Table 3. Decarboxylation of Biomass-Derived Substrates to MAA with the $\text{BaAl}_{12}\text{O}_{19}$ Catalyst

entry ^a	substrates	conversion (%)	selectivity (mol %)			
			MAA	2-HIBA	AA	others ^b
1	itaconic acid	100	50	18	3	29
2	citric acid	100	50	16	6	28
3	aconitic acid	85	51	18	4	27

^aReaction conditions: substrate (2 g), solvent (water, 150 mL), time (3 h), catalyst (1 g), temperature (250 °C), and pressure (20 bar).

^bOthers = pyruvic acid, crotonic acid, acetone, propene, and carbon dioxide. Values were determined by HPLC. IA is itaconic acid, MAA is methacrylic acid, AA is acetic acid, and 2-HIBA is 2-hydroxyisobutyric.

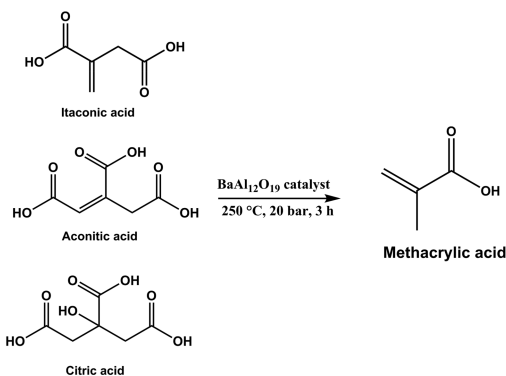
We have started our experiment with citric acid, one of the most versatile and widely available biomolecule industrially produced by the fermentation of various carbohydrate sources.³⁰ It can also be upgraded to IA by the surface fermentation process.³¹ In our approach, we have achieved a good MAA yield by the dehydration and decarboxylation of citric acid. Interestingly, the $\text{BaAl}_{12}\text{O}_{19}$ catalyst also demonstrates high activity, enabling a maximum 50% yield of MAA under mild reaction conditions (Table 3, entry 2). Similarly, decarboxylation of aconitic acid (dehydration product of citric acid) using the $\text{BaAl}_{12}\text{O}_{19}$ catalyst gave 51% yield of MAA (Table 3, entry 3).

We have also performed the catalyst reusability experiment to test the stability of the $\text{BaAl}_{12}\text{O}_{19}$ catalyst under hydrothermal conditions (Table 2, entry 4). We have washed the reused catalyst after each run with distilled water and acetone and dried in an oven at 60 °C. We have not added fresh catalyst in the reaction mixture to compensate any mass loss during the catalyst washing procedure. It was found that the yield of MAA decreased from 50 to 43% after four consecutive cycles (Figure S5). This could be attributed to the mass loss (7%) of the catalyst during the washing procedure.²⁹

3.2. Synthesis and Characterization of the Poly(St-co-BA-co-MAA)copolymer Latexes. In collaboration with HELIOS, one of the world's leading paint and coating producers, we have used the as-synthesized biobased MAA to prepare the poly(St-co-BA-co-MAA) copolymer. The copolymer was synthesized by emulsion polymerization of styrene and biobased MAA in butyl acrylate with *tert*-butyl peroxybenzoate as the initiator (Figure 1). We have also compared the latex properties of the bio-MAA-based copolymer with the commercial poly(St-co-BA-co-MAA) copolymer derived from petroleum-based MAA.

The ¹H NMR spectrum of the copolymer (Figure 2) shows aromatic ring proton signals of styrene at around 6.5–7.4 ppm (peak a). The peak around 3.7–4.1 ppm (peak f) corresponds to the hydrogens of the methylene located next to the ester group. The peak “b” at a chemical shift of around 0.7–0.9 ppm was assigned to the methyl groups of the MAA. The peaks around 1.4–2.1 ppm (c, c', d, e) correspond to the –CH and

Monomer Synthesis



Copolymer Synthesis

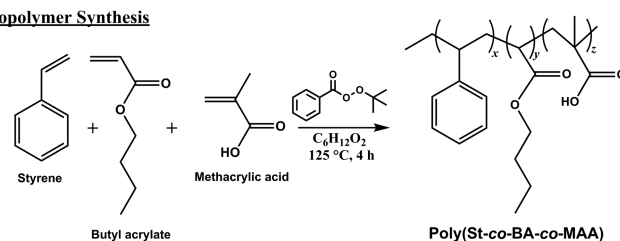


Figure 1. Schematic illustrating the monomer and copolymer synthesis processes for producing biomass-derived MAA-based poly(St-co-BA-co-MAA).

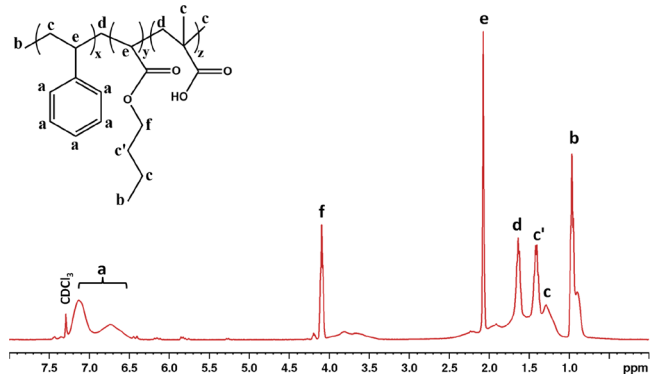


Figure 2. ¹H NMR spectrum obtained for the bio-MAA-based poly(St-co-BA-co-MAA) copolymer.

–CH₂ backbone of poly(styrene), poly(butyl acrylate), and poly(methacrylic acid), respectively.

The FT-IR spectrum of the copolymer confirmed the successful polymerization of the MAA monomer into a copolymer structure (Figure 3). The characteristic peak at 1634 cm^{-1} in the absorption pattern related to the carboxylic groups. The aromatic carbon double bond (C=C) at 1460 cm^{-1} , C–H out-of-plane bending vibration at 696 cm^{-1} , and the C–O–C bond at 1160 cm^{-1} represents the butyl acrylate and styrene segments within the copolymer chain, respectively.^{32–34}

GPC analysis was carried out to assess polydispersity and to allow comparison of the bio-MAA-based copolymer and petroleum-derived MAA-based copolymer. According to the GPC results (Table S3), the apparent average molecular weight (M_n) of the biocopolymer is slightly lower than that of the copolymer prepared from petroleum-based monomers. The slightly higher molecular weight of the petroleum-based copolymer could be associated with the formation of gel during emulsion polymerization.⁶ Nevertheless, slightly narrower

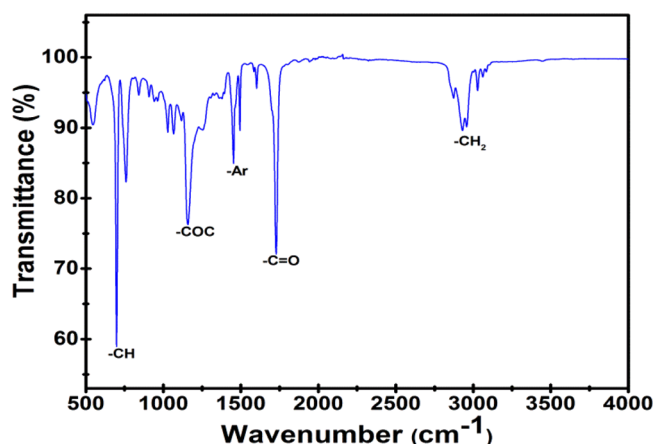


Figure 3. FT-IR spectra of bio-MAA-based poly(St-co-BA-co-MAA) with assigned characteristic peaks.

molecular weight distribution (MWD) at the biocopolymer is favorable in almost all types of coatings.³⁵ The polydispersity indexes ($PDI = M_w/M_n$) of copolymers are in the range of 1.45–1.54. Such a broad MWD confirmed that along with the chain transfer to the chain transfer agent, transfer to the polymer has also been the main termination event.³⁶ According to the GPC traces in Figure 4, the MWDs of both copolymers were in good agreement.

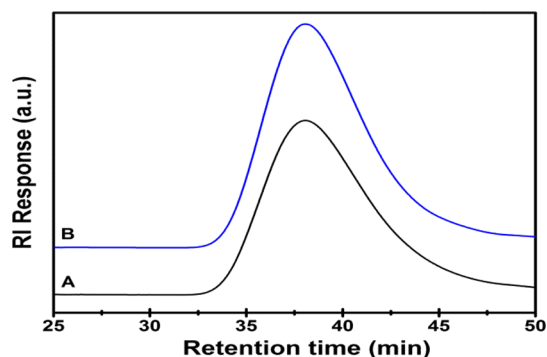


Figure 4. GPC spectra of bio-MAA-based (A) and petroleum-derived MAA-based (B) poly(St-co-BA-co-MAA) copolymers.

The stabilities of as-synthesized copolymers at high temperature were evaluated by DSC and TGA. Table S3 shows the results of TGA for copolymers, and it was found that both biobased and petroleum-based copolymers are thermally stable. The TGA of copolymers showed two-step decomposition regions (Figure 5). The first weight loss region (10% weight loss) at around 250–280 °C (T_{10}) may be because of the decarboxylation and/or other reactions of side-chain units.³⁷ The secondary exo-effects occurred at around 400 °C (T_d) with maximum decomposition (62% weight loss) of copolymers. This could be due to the decomposition of side chain or from the scission of the random chain in the backbone.³⁸

Furthermore, according to the DSC measurements both the copolymers showed only one glass transition region ($T_g = \sim 24$ °C). This phenomena suggested that both copolymers follow a monomer-starved semibatch feed policy that produces copolymers with homogeneous compositions (Table S3, Figure 6).³⁹

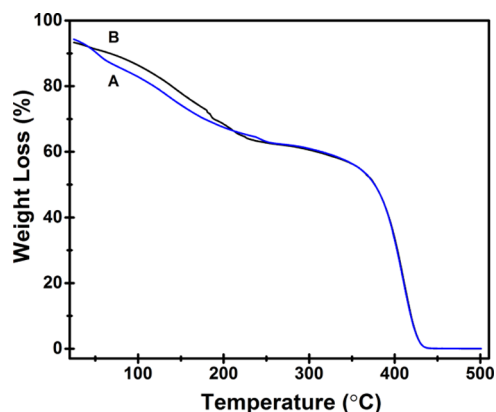


Figure 5. TGA thermograms of weight change as a function of temperature for bio-MAA-based (A) and petroleum-derived MAA-based (B) poly(St-co-BA-co-MAA) copolymers.

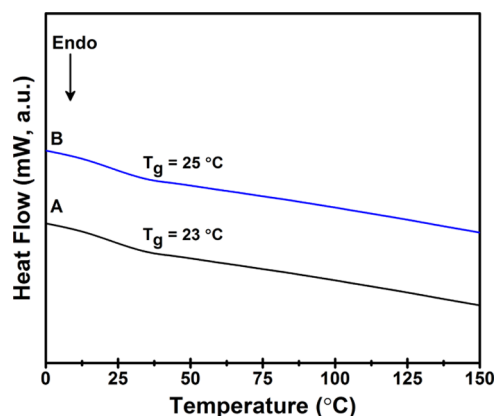


Figure 6. DSC thermograms for bio-MAA-based (A) and petroleum-derived MAA-based (B) poly(St-co-BA-co-MAA) copolymers.

We have studied the shear viscosity of biobased and petroleum-based copolymers, which were dependent on the shear rate.

The viscosity of the copolymer is an important property that decides the quality of the final industrial product. It was observed that when the shear rate increased or decreased, viscosity behavior of petroleum-based and biobased copolymers remained almost constant. Newtonian viscosity behavior between 4.50 and 6.50 Pa s at 25 °C laid a good foundation for usage in coating applications. The conventional polymerization with a high solid content (>60%), low viscosity and with film-forming ability can be obtained for the emulsion polymerization. Table S4 compares technical data sheet parameters required for the formulation of synthetic resin in the industries. As evident, all the requirements are met. The solid content and viscosity similarity promises practically the same application properties of the paint.

As can be observed from Figure 7, both polymer solutions exhibit the Newtonian behavior, which is well-known characteristic for solvent solutions.⁴⁰ Pendant carboxyl groups are important adhesion promoters via hydrogen-bonding mechanism between the substrate and coating.⁴¹ Because of the only source of -COOH groups in a formulation of MAA, comparable adhesion is expected. The importance of the color index is governed with the shade of the coating.

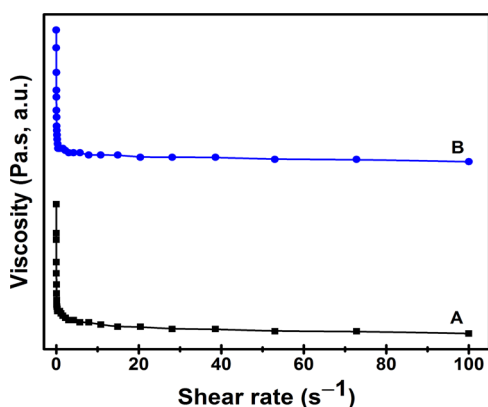


Figure 7. Viscosity obtained at 25 °C for bio-MAA-based (A) and petroleum-derived MAA-based (B) poly(St-co-BA-co-MAA) copolymers.

4. CONCLUSIONS

In summary, we have prepared biomass-derived MAA from IA, citric acid, and aconitic acid by using variety of heterogeneous catalysts. Besides the conventional noble metal-based catalysts, a series of heterogeneous acid and base catalysts were screened. Among different heterogeneous catalysts, the $\text{BaAl}_{12}\text{O}_{19}$ catalyst exhibited superior activity, giving a maximum 50% yield of MAA under mild reaction conditions.

Furthermore, biobased citric acid and aconitic acid were successfully converted to MAA in one-pot reaction over the $\text{BaAl}_{12}\text{O}_{19}$ catalyst. Further, the biobased MAA used for its radical polymerizations afforded partially biobased copolymers with a good control of M_n and moderate PDI values. The poly(St-co-BA-co-MAA) copolymer produced from biobased MAA showed thermal stability, T_g values of around 26 °C, which are similar to the petroleum-based copolymer. The shear flow of copolymers whereas Newtonian viscosity behavior between 4.50 and 6.50 Pa s at 25 °C laid a good foundation for usage in coating applications.

■ ASSOCIATED CONTENT

Supporting Information

The Supporting Information is available free of charge on the ACS Publications website at DOI: 10.1021/acs.iecr.9b04057.

Experimental details, characterizations of the catalysts (XRD, transmission electron microscopy, Brunauer–Emmett–Teller, acidity/basicity results) and copolymer (GPC, ^1H and ^{13}C NMR) (PDF)

■ AUTHOR INFORMATION

Corresponding Authors

*E-mail: ashish.bohre@ki.si. Phone: +386 1 4760504. Fax: +386 1 4760300 (A.B.).

*E-mail: blaz.likozar@ki.si (B.L.).

ORCID

Ashish Bohre: 0000-0002-5594-9753

Mohammad Asif Ali: 0000-0002-5717-5659

Miha Grilc: 0000-0002-8255-647X

Blaž Likozar: 0000-0001-9194-6595

Notes

The authors declare no competing financial interest.

■ ACKNOWLEDGMENTS

The authors thank the Slovenian Research Agency (research core funding no. P2–0152) for the financial support. The research was also supported by the RDI project Cel. The cycle entitled “Potential of biomass for development of advanced materials and biobased products”, which is cofinanced by the Ministry of Education, Science and Sport, Republic of Slovenia, and the European Union through the European Regional Development Fund, 2016–2020.

■ REFERENCES

- (1) Fernández-García, M.; Fernández-Sanz, M.; López Madruga, E.; Fernández-Monreal, C. A kinetic study of free radical copolymerization of styrene/butyl acrylate. *Macromol. Chem. Phys.* **1999**, *200*, 199–205.
- (2) Kammona, O.; Pladis, P.; Frantzikinakis, C. E.; Kiparissides, C. A comprehensive experimental and theoretical investigation of the styrene/2-ethylhexyl acrylate emulsion copolymerization. *Macromol. Chem. Phys.* **2003**, *204*, 983–999.
- (3) Hamzehlou, S.; Reyes, Y.; Hutchinson, R.; Leiza, J. R. Copolymerization of n-Butyl Acrylate and Styrene: Terminal vs Penultimate Model. *Macromol. Chem. Phys.* **2014**, *215*, 1668–1678.
- (4) Chern, C. S. Emulsion polymerization mechanisms and kinetics. *Prog. Polym. Sci.* **2006**, *31*, 443–486.
- (5) Naghash, H. J.; Karimzadeh, A.; Massah, A. R. Synthesis and properties of styrene–butylacrylate emulsion copolymers modified by silane compounds. *J. Appl. Polym. Sci.* **2009**, *112*, 1037–1044.
- (6) Hua, H.; Dubé, M. A. Semi-continuous emulsion copolymerization of styrene-butyl acrylate with methacrylic acid: screening design of experiments. *Polym.-Plast. Technol. Eng.* **2011**, *50*, 349–361.
- (7) Tripathi, A. K.; Tsavalas, J. G.; Sundberg, D. C. Partitioning of functional monomers in emulsion polymerization: distribution of carboxylic acid monomers between water and monomer phases. *Ind. Eng. Chem. Res.* **2014**, *53*, 6600–6612.
- (8) Tripathi, A. K.; Sundberg, D. C. Partitioning of functional monomers in emulsion polymerization: distribution of carboxylic acid monomers between water and multimonomer systems. *Ind. Eng. Chem. Res.* **2013**, *52*, 9763–9769.
- (9) Santos, A. M.; Guillot, J.; McKenna, T. F. Partitioning of styrene, butyl acrylate and methacrylic acid in emulsion systems. *Chem. Eng. Sci.* **1998**, *53*, 2143–2151.
- (10) Oliveira, M. P. d.; Silva, C. R.; Guerrini, L. M. Effect of itaconic acid on the wet scrub resistance of highly pigmented paints for architectural coatings. *J. Coat. Technol. Res.* **2011**, *8*, 439–447.
- (11) Montano, V.; Smits, A.; Garcia, S. J. The bio-touch: Increasing coating functionalities via biomass-derived components. *Surf. Coat. Technol.* **2018**, *341*, 2–14.
- (12) Webster, O. W. The discovery and commercialization of group transfer polymerization. *J. Polym. Sci., Part A: Polym. Chem.* **2000**, *38*, 2855–2860.
- (13) Wang, R.; Zhang, J.; Kang, H.; Zhang, L. Design, preparation and properties of bio-based elastomer composites aiming at engineering applications. *Compos. Sci. Technol.* **2016**, *133*, 136–156.
- (14) Li, J.; Brill, T. B. Spectroscopy of hydrothermal solutions 18: pH-dependent kinetics of itaconic acid reactions in real time. *J. Phys. Chem. A* **2001**, *105*, 10839–10845.
- (15) Yasuda, S.; Iwakura, A.; Hirata, J.; Kanno, M.; Ninomiya, W.; Otomo, R.; Kamiya, Y. Strong Brønsted acid-modified chromium oxide as an efficient catalyst for the selective oxidation of methacrolein to methacrylic acid. *Catal. Commun.* **2019**, *125*, 43–47.
- (16) Mahboub, M. J. D.; Dubois, J.-L.; Cavani, F.; Rostamizadeh, M.; Patience, G. S. Catalysis for the synthesis of methacrylic acid and methyl methacrylate. *Chem. Soc. Rev.* **2018**, *47*, 7703–7738.
- (17) Mahboub, M. J. D.; Lotfi, S.; Dubois, J.-L.; Patience, G. S. Gas phase oxidation of 2-methyl-1, 3-propanediol to methacrylic acid over heteropolyacid catalysts. *Catal. Sci. Technol.* **2016**, *6*, 6525–6535.

- (18) Nagai, K.; Ui, T. *Trends and Future of Monomer-MMA Technologies*; Sumitomo Chemicals, 2004; Vol 2, pp 4–13.
- (19) Pyo, S.-H.; Dishisha, T.; Dayankac, S.; Gerelsaikhan, J.; Lundmark, S.; Rehnberg, N.; Hatti-Kaul, R. A new route for the synthesis of methacrylic acid from 2-methyl-1, 3-propanediol by integrating biotransformation and catalytic dehydration. *Green Chem.* **2012**, *14*, 1942–1948.
- (20) Le Nôtre, J.; Witte-van Dijk, S. C. M.; van Haveren, J.; Scott, E. L.; Sanders, J. P. M. Synthesis of Bio-Based Methacrylic Acid by Decarboxylation of Itaconic Acid and Citric Acid Catalyzed by Solid Transition-Metal Catalysts. *ChemSusChem* **2014**, *7*, 2712–2720.
- (21) Pirmoradi, M.; Kastner, J. R. Synthesis of Methacrylic Acid by Catalytic Decarboxylation and Dehydration of Carboxylic Acids Using a Solid Base and Subcritical Water. *ACS Sustainable Chem. Eng.* **2016**, *5*, 1517–1527.
- (22) Kumar, S.; Krishnan, S.; Samal, S. K.; Mohanty, S.; Nayak, S. K. Itaconic acid used as a versatile building block for the synthesis of renewable resource-based resins and polyesters for future prospective: a review. *Polym. Int.* **2017**, *66*, 1349–1363.
- (23) Apelblat, A. *Citric Acid*; Springer, 2014.
- (24) Ali, S. H.; Al-Rashed, O.; Azeez, F. A.; Merchant, S. Q. Potential biofuel additive from renewable sources—kinetic study of formation of butyl acetate by heterogeneously catalyzed transesterification of ethyl acetate with butanol. *Bioresour. Technol.* **2011**, *102*, 10094–10103.
- (25) Lian, J.; McKenna, R.; Rover, M. R.; Nielsen, D. R.; Wen, Z.; Jarboe, L. R. Production of biorenewable styrene: utilization of biomass-derived sugars and insights into toxicity. *J. Ind. Microbiol. Biotechnol.* **2016**, *43*, 595–604.
- (26) Bohre, A.; Hočevar, B.; Grilc, M.; Likozar, B. Selective catalytic decarboxylation of biomass-derived carboxylic acids to bio-based methacrylic acid over hexaaluminate catalysts. *Appl. Catal., B* **2019**, *256*, 117889.
- (27) Lee, H.; Juan, J.; Binti Abdullah, N.; Nizah MF, R.; Taufiq-Yap, Y. Heterogeneous base catalysts for edible palm and non-edible Jatropha-based biodiesel production. *Chem. Cent. J.* **2014**, *8*, 30.
- (28) De Schouwer, F.; Claes, L.; Claes, N.; Bals, S.; Degève, J.; De Vos, D. E. Pd-catalyzed decarboxylation of glutamic acid and pyroglutamic acid to bio-based 2-pyrrolidone. *Green Chem.* **2015**, *17*, 2263–2270.
- (29) Tian, M.; Wang, X. D.; Zhang, T. Hexaaluminates: a review of the structure, synthesis and catalytic performance. *Catal. Sci. Technol.* **2016**, *6*, 1984–2004.
- (30) Alben, E.; Erkmen, O. Production of citric acid from a new substrate, undersized semolina, by *Aspergillus niger*. *Food Technol. Biotechnol.* **2004**, *42*, 19–22.
- (31) Verduyck, J.; De Vos, D. E. Highly selective one-step dehydration, decarboxylation and hydrogenation of citric acid to methylsuccinic acid. *Chem. Sci.* **2017**, *8*, 2616–2620.
- (32) Rufino, E. S.; Monteiro, E. E. C. Infrared study on methyl methacrylate–methacrylic acid copolymers and their sodium salts. *Polymer* **2003**, *44*, 7189–7198.
- (33) Mohamadian, N.; Ghorbani, H.; Wood, D. A.; Khoshmardan, M. A. A hybrid nanocomposite of poly (styrene-methyl methacrylate-acrylic acid)/clay as a novel rheology-improvement additive for drilling fluids. *J. Polym. Res.* **2019**, *26*, 33.
- (34) Gonçalves, M. A.; Pinto, V. D.; Dias, R. C.; Costa, M. R. P. *FTIR-ATR Monitoring and SEC/RI/MALLS Characterization of ATRP Synthesized Hyperbranched Polyacrylates, Macromolecular Symposia*; Wiley Online Library, 2010; pp 210–228.
- (35) Qi, Y.; Li, L.; Fang, Z.; Zhong, J.; Dong, Q. Effects of small molecular weight silicon-containing acrylate on kinetics, morphologies, and properties of free-radical/cationic hybrid UV-cured coatings. *J. Appl. Polym. Sci.* **2014**, *131*, 40655.
- (36) Sayer, C.; Lima, E. L.; Pinto, J. C.; Arzamendi, G.; Asua, J. M. Kinetics of the seeded semicontinuous emulsion copolymerization of methyl methacrylate and butyl acrylate. *J. Polym. Sci., Part A: Polym. Chem.* **2000**, *38*, 367–375.
- (37) Naghash, H. J.; Karimzadeh, A.; Momeni, A. R.; Massah, A. R.; Alian, H. Preparation and properties of triethoxyvinylsilane-modified styrene-butyl acrylate emulsion copolymers. *Turk. J. Chem.* **2007**, *31*, 257–269.
- (38) Ai, Z.-Q.; Zhou, Q.-L.; Xie, C.-S.; Zhang, H.-T. In situ preparation and properties of high-solid-content and low-viscosity poly (methyl methacrylate/n-butyl acrylate/acrylic acid)/poly (styrene/acrylic acid) composite latexes. *J. Appl. Polym. Sci.* **2007**, *103*, 1815–1825.
- (39) Rios, L.; Hidalgo, M.; Cavaille, J. Y.; Guillot, J.; Guyot, A.; Pichot, C. Polystyrene (1)/poly (butyl acrylate-methacrylic acid)(2) core-shell emulsion polymers. Part I. Synthesis and colloidal characterization. *Colloid Polym. Sci.* **1991**, *269*, 812–824.
- (40) Macosko, C. W.; Larson, R. G. *Rheology: Principles, Measurements, and Applications*; VCH, 1994.
- (41) Paul, S. *Surface Coatings*; Science and technology, 1985.